Isopiestic Determination of the Activity Coefficients of Some Aqueous Rare Earth Electrolyte Solutions at 25 °C. 4. $La(NO_3)_3$, $Pr(NO_3)_3$, and $Nd(NO_3)_3$

Joseph A. Rard*† and Donald G. Miller

University of California, Lawrence Livermore Laboratory, Livermore, California 94550

Frank H. Spedding

Ames Laboratory—U.S. Department of Energy and Department of Chemistry, Iowa State University, Ames, Iowa 50011

The osmotic coefficients of aqueous $La(NO_3)_3$, $Pr(NO_3)_3$, and $Nd(NO_3)_3$ solutions have been measured from 0.1 mol kg^{-1} to 6.2–6.4 mol kg^{-1} at 25 °C by using the isopiestic method. The resulting osmotic coefficients were fitted to semiempirical least-squares equations, and these equations were used to calculate water activities and mean molal activity coefficients. The data up to 2.0 mol kg^{-1} were also fitted to Pitzer's equation. These data are compared to other available thermodynamic and transport data for rare earth electrolyte solutions.

Introduction

Activity coefficient data have recently been reported for rare earth chloride (*30*), perchlorate (*20*), and nitrate solutions (*18*) at 25 °C. The water activities of the rare earth chlorides and perchlorates at low and moderate concentrations form S-shaped curves as a function of the ionic radius, and these series trends were interpreted as being mainly due to trends in the cation hydration (*18*, *20*, *30*). Data have been published for six rare earth nitrates up to saturation (or supersaturation). However, only a few points were measured for the light rare earth nitrates. The available rare earth nitrate activity data appear to be showing significantly different series trends from the rare earth chlorides and perchlorates.

Various thermodynamic (*2*, *26*, *28*, *32*) and transport properties (*19*, *29*) for these salts indicate that the rare earth ionic hydration trends are significantly modified by interactions with the nitrate ions. Spectral studies (*1*, *3*, *5*, *6*, *9*, *14*, *21–25*) suggest that complex formation is predominantly, or entirely, solvent separated in rare earth chloride and perchlorate solutions, but both inner- and outer-sphere complexes are formed in rare earth nitrate solutions. Activity data for the remaining rare earth nitrate solutions are desirable both for their own intrinsic value and for the information they yield about complex formation in solution. In this paper isopiestic data are reported for $La(NO_3)_3$, $Pr(NO_3)_3$, and $Nd(NO_3)_3$ solutions from 0.1 mol kg^{-1} to supersaturated concentrations.

Experimental Section

The isopiestic chambers and experimental techniques have been described in detail (*18*, *20*, *30*) so only a few comments are necessary here. All of the isopiestic measurements were made at 25.00 ± 0.01 °C (IPTS-68), and the isopiestic molalities are reported in terms of IUPAC-1969 atomic weights. The isopiestic standards were KCl and $CaCl_2$ solutions. Isopiestic equilibration times for rare earth nitrate concentrations above 0.6 mol kg^{-1} were for 4–12 days, while 3–5 weeks were used at lower concentrations. Each equilibration involved duplicate samples of each solution, and averaged molalities are reported. Equilibrium was approached from both higher and lower concentrations. The individual isopiestic molalities of each salt, for rare earth nitrate concentrations above 0.3 mol kg^{-1}, agreed to within ±0.1% of the average, while in most cases the agreement was to within ±0.05%. At lower concentrations ±0.15% was considered acceptable. The rare earth nitrate solutions were adjusted to their equivalence pH values and then analyzed by EDTA titrations and the gravimetric sulfate method (after destroying the nitrate ions by evaporation with HCl). The stock solution concentrations were known to 0.1% or better. The solution preparation and analyses were performed by one of us while at the Ames Laboratory, and the isopiestic equilibrations were later made at Lawrence Livermore Laboratory.

The $CaCl_2$ isopiestic standard stock solution that was used for the present measurements was also used for all of our previous measurements (*17*, *18*, *20*, *30*), with the exception of a few of the KCl–$CaCl_2$ points and about half of the rare earth chloride points (*17*, *30*). This $CaCl_2$ stock solution had been analyzed several years ago by the gravimetric sulfate method and a concentration of 6.6262 ± 0.0004 mol kg^{-1} was obtained (triplicate analysis). After the presently reported isopiestic measurements were completed, this stock solution was reanalyzed by the same method and the $CaCl_2$ concentration was found to be 6.6263 ± 0.0019 mol kg^{-1}.

Calculations and Errors

The osmotic coefficients of the rare earth nitrate solutions were calculated from

$$\Phi = \nu^*\Phi^* m^*/\nu m \qquad (1)$$

where m is the molal concentration of the rare earth nitrate solution, $\nu = 4$ is the number of ions formed by the complete dissociation of one molecule of rare earth nitrate, and Φ is the molal osmotic coefficient of the rare earth nitrate solution. The equivalent quantities for the reference solutions are indicated with an asterisk. The reference solution osmotic coefficients were calculated from available equations (*8*, *17*). The isopiestic molalities and the reference solution osmotic coefficients are given in Tables I and II.

The osmotic coefficients for each rare earth nitrate solution were fitted to the equation

$$\Phi = 1 - (A/3)m^{1/2} + \sum_i A_i m^{r_i} \qquad (2)$$

where $A = 8.6430$ for 3–1 electrolytes. The r_i were not constrained to form a consecutive sequence. All of the osmotic coefficients from this research were given unit weights for eq 2, as were the $La(NO_3)_3$ and $Pr(NO_3)_3$ values reported earlier

† Visiting Assistant Professor of Geology 1977–1978, University of Illinois at Urbana—Champaign, tenure served as participating guest at Lawrence Livermore Laboratory. Address correspondence to author at Lawrence Livermore Laboratory.

0021-9568/79/1724-0348$01.00/0

Table I. Isopiestic Molalities of Some Rare Earth Nitrate Solutions from Measurements with KCl Reference Solutions

$[La(NO_3)]$, m	$[Pr(NO_3)_3]$, m	$[Nd(NO_3)_3]$, m	[KCl], m	Φ(KCl)
0.124 81	0.125 53	0.126 78	0.205 04	0.9120
0.129 90	0.130 33	0.131 51	0.212 49	0.9114
0.296 28	0.297 89	0.300 66	0.501 76	0.8992
0.389 07	0.390 28	0.392 33	0.670 18	0.8972
0.396 26	0.397 30	0.399 48	0.683 41	0.8971
0.464 71	0.465 20	0.467 02	0.810 30	0.8968
0.571 20	0.570 08	0.571 19	1.014 7	0.8974
0.663 54	0.660 22	0.660 70	1.195 9	0.8989
0.741 63	0.736 59	0.736 14	1.353 8	0.9006
0.847 94	0.839 66	0.838 18	1.573 6	0.9037
0.946 90	0.934 92	0.932 47	1.783 7	0.9072
1.035 9	1.020 9	1.017 1	1.975 5	0.9108
1.174 0	1.153 9	1.147 8	2.280 6	0.9173
1.210 0	1.188 3	1.181 6	2.364 1	0.9192

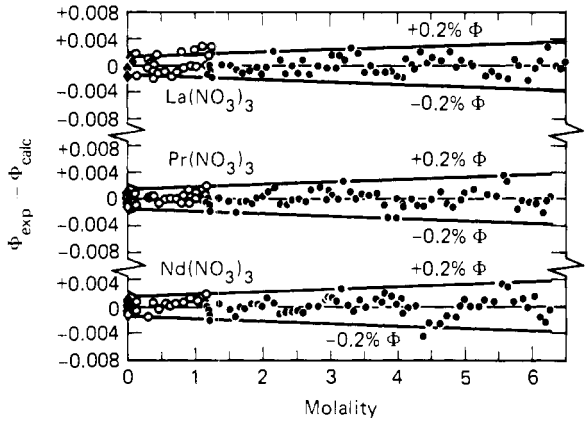

Figure 1. Differences between experimental and calculated osmotic coefficients of $La(NO_3)_3$, $Pr(NO_3)_3$, and $Nd(NO_3)_3$ at 25 °C: (●) isopiestic vs. $CaCl_2$; (O) isopiestic vs. KCl; (♦) freezing point depression; (◇) estimated from electrical conductances.

(*18*). Dilute solution freezing point depression data for $La(NO_3)_3$ and $Pr(NO_3)_3$ (*7*, *10*), measured early this century, were converted to osmotic coefficients at 25 °C by using available thermal data (*2*, *26*, *32*); these osmotic coefficients for $La(NO_3)_3$ were given weights of 1 or 0 in the least-squares fits. Most of the $Pr(NO_3)_3$ freezing point data (*10*) are significantly lower than the isopiestic results so they were not included in the least-squares fits. The samples of rare earths available early this century were usually of low purity so this discrepancy is not really surprising. No reliable dilute solution data were available for $Pr(NO_3)_3$ or $Nd(NO_3)_3$, so values of Φ for these salts below 0.1 mol kg^{-1} were estimated from ion size parameters obtained from electrical conductance data (*18*). These estimated Φ values were also given unit weights. The best values of A_i and r_i are listed in Table III, along with the standard deviation of each fit. The differences between the experimental and calculated osmotic coefficients are illustrated in Figure 1. Nearly all of the data fall within 0.2% of eq 2 and most of the points are within 0.1%.

If eq 2 is substituted into the Gibbs–Duhem equation, then

$$\ln \gamma_{\pm} = -Am^{1/2} + \sum_i A_i \frac{(r_i + 1)}{r_i} m^{r_i} \qquad (3)$$

where $\gamma_{\pm}$ is the mean molal activity coefficient of the salt and the $-Am^{1/2}$ term is the Debye–Hückel limiting law. Values of Φ, $\gamma_{\pm}$, and a_1 (water activity) are given in Table IV, at various molalities. The osmotic coefficients up to 2.0 mol kg^{-1} were also fitted to Pitzer's equation. The paper of Pitzer et al. (*16*) should be consulted for the meaning of the various parameters. Following Pitzer et al. (*16*), we have held $3\beta^{(1)}/2$ fixed at 7.70 and have also used the Pitzer et al. weights for the data points.

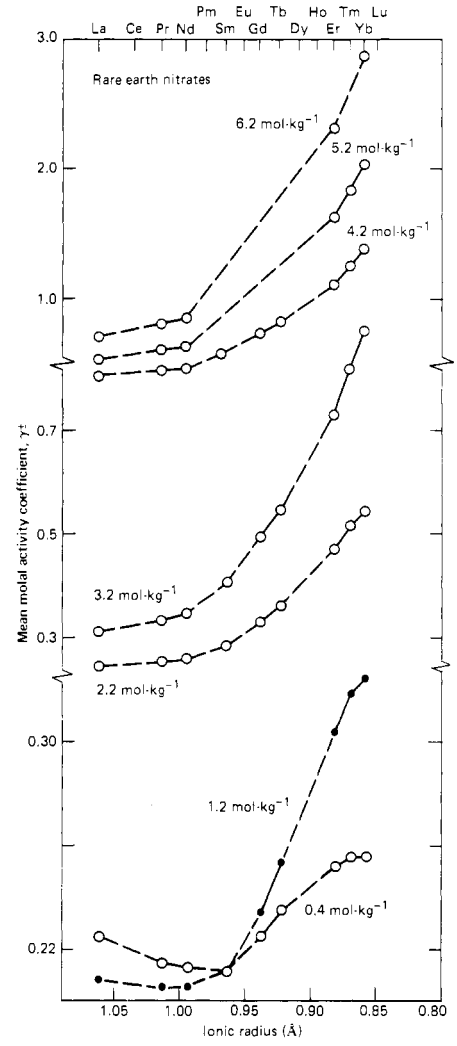

Figure 2. Mean molal activity coefficients of rare earth nitrate solutions at constant molalities.

The parameters of Pitzer's equation are given in Table V. Equations 2 and 3 should be used if highly accurate values are needed for Φ and $\gamma_{\pm}$.

The maximum expected errors for the experimental osmotic coefficients are 0.3%, while the probable errors are around 0.2%. The data of this research for $La(NO_3)_3$ connect up fairly smoothly with osmotic coefficients obtained from freezing point depression measurements. However, the $La(NO_3)_3$ osmotic coefficients of Kirgintsev and Luk'yanov (*11*) are about 1% lower than the values reported here. They stated that they analyzed their $La(NO_3)_3$ stock solution concentration by the sulfate method but gave no details about the analysis. Presumably, they used

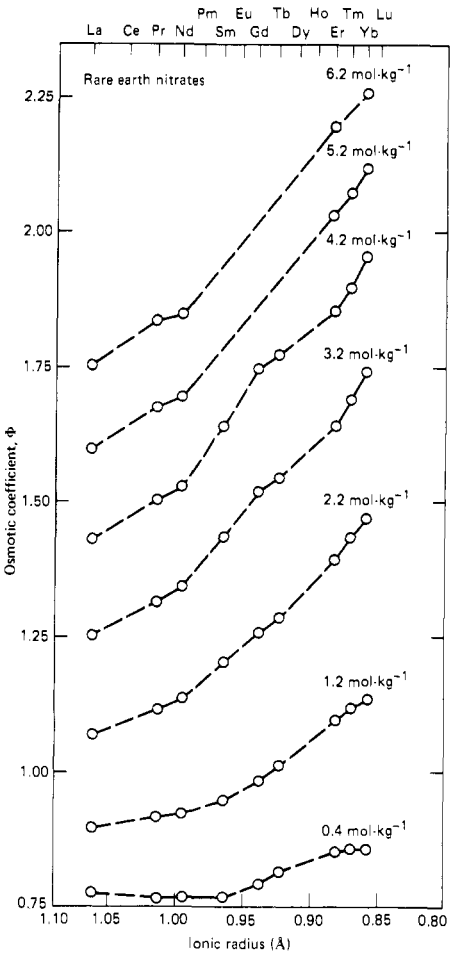

Figure 3. Osmotic coefficients of rare earth nitrate solutions at constant molalities.

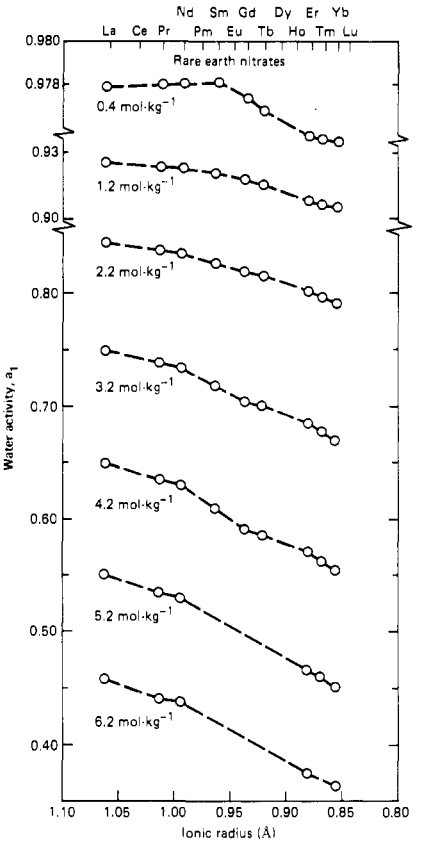

Figure 4. Water activities of rare earth nitrate solutions at constant molalities.

direct addition of H_2SO_4 to samples of the stock solution. This may result in nitrate ion coprecipitation and gives low apparent values for the osmotic coefficients (*18*).

Results

Figures 2–4 are constant molality plots of $\gamma_{\pm}$, Φ, and a_1, as a function of the ionic radius (*31*), for the rare earth nitrates. At low concentrations the water activities increase slightly from $La(NO_3)_3$ to $Sm(NO_3)_3$ and then decrease to $Yb(NO_3)_3$, while at higher concentrations the water activities decrease from $La(NO_3)_3$ to $Yb(NO_3)_3$. From about 3.0 mol kg^{-1} to higher concentrations, there is a downward "bulge" in the middle of the series. The series curves for $\gamma_{\pm}$ and Φ exhibit trends similar to a_1 but in the reverse direction.

The series trends for the nitrates differ significantly from those found for the rare earth chlorides and perchlorates. The series trends for ln $\gamma_{\pm}$ and a_1 are shown in Figures 5 and 6 for these three anion series at 3.4 mol kg^{-1}. It is clear that there is a large anion shift for both of these properties along with a smaller radius-dependent trend for each anion series. The rare earth chloride and perchlorate $\gamma_{\pm}$ and a_1 values show considerable qualitative similarity. For example, a_1 decreases from La to Nd and from Sm to Lu, with the data for Sm to Lu displaced relative to the light rare earths. A displacement also occurs in the middle of the series for the rare earth nitrates but in the reverse direction. In contrast, at low concentrations the $\gamma_{\pm}$ and a_1 series curves for the chlorides and perchlorates are S shaped.

The S shape of the rare earth chloride and perchlorate activities at constant low molalities has been interpreted as being mainly due to two factors related to cation hydration trends (*20*). The first factor is the increase in cation hydration from La to

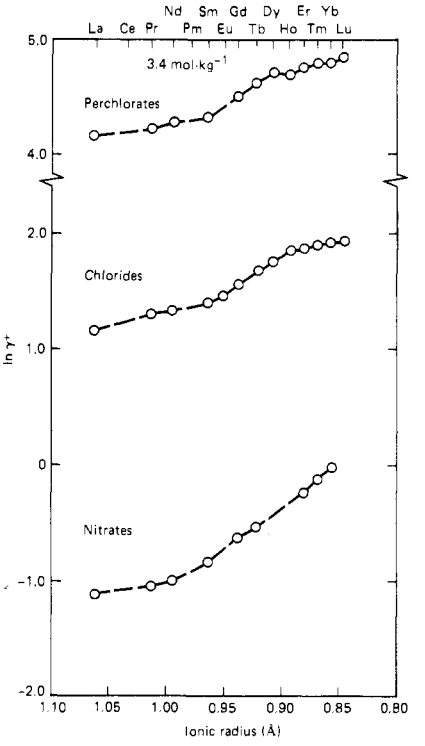

Figure 5. Natural logarithm of the mean molal activity coefficients of rare earth chlorides, perchlorates, and nitrates at 3.4 mol kg^{-1}.

Lu due to the increase in the cation surface charge density as the lanthanide contraction occurs. The second effect is a proposed decrease in the inner-sphere hydration number between Nd and Tb, as a consequence of the decreasing cation size. Detailed descriptions of the effect of these hydration changes on thermodynamic properties have been given else-

Table II. Isopiestic Molalities of Some Rare Earth Nitrate Solutions from Measurements with $CaCl_2$ Reference Solutions

$[La(NO_3)_3]$, m	$[Pr(NO_3)_3]$, m	$[Nd(NO_3)_3]$, m	$[CaCl_2]$, m	$\Phi(CaCl_2)$
1.1836	1.1629	1.1565	1.2564	1.1196
1.2001	1.1794	1.1727	1.2733	1.1249
1.2230	1.2017	1.1949	1.2947	1.1317
1.2494	1.2269	1.2194	1.3186	1.1393
1.3969	1.3675	1.3569	1.4587	1.1849
1.5397	1.5043	1.4914	1.5903	1.2293
1.6413	1.6026	1.5865	1.6822	1.2611
1.7186	1.6742	1.6571	1.7515	1.2855
1.8003	1.7525	1.7337	1.8250	1.3118
1.8947	1.8435	1.8217	1.9094	1.3423
1.9675	1.9110	1.8883	1.9724	1.3654
2.0566	1.9971	1.9735	2.0519	1.3949
2.1541	2.0926	2.0666	2.1395	1.4278
2.2562	2.1883	2.1617	2.2266	1.4609
2.3405	2.2694	2.2403	2.2962	1.4876
2.4357	2.3581	2.3271	2.3751	1.5181
2.5233	2.4442	2.4119	2.4518	1.5480
2.6205	2.5407	2.5066	2.5367	1.5814
2.7060	2.6197	2.5846	2.6053	1.6086
2.8244	2.7335	2.6975	2.7061	1.6488
2.9624	2.8655	2.8281	2.8198	1.6946
3.0547	2.9595	2.9172	2.8982	1.7263
3.1004	2.9989	2.9571	2.9329	1.7404
3.1431	3.0444	3.0009	2.9706	1.7558
3.2309	3.1293	3.0845	3.0413	1.7846
3.3209	3.2143	3.1707	3.1164	1.8154
3.4111	3.3030	3.2599	3.1885	1.8451
3.5096	3.3951	3.3508	3.2634	1.8759
3.6037	3.4866	3.4401	3.3399	1.9075
3.7056	3.5844	3.5386	3.4201	1.9407
3.8522	3.7260	3.6785	3.5365	1.9889
3.9276	3.8022	3.7521	3.5962	2.0137
4.0055	3.8796	3.8240	3.6563	2.0386
4.0960	3.9675	3.9123	3.7271	2.0680
4.1447	4.0142		3.7693	2.0854
		3.9826	3.7823	2.0908
4.2220	4.0897	4.0395	3.8288	2.1101
4.2327	4.0982		3.8359	2.1130
		4.0624	3.8442	2.1164
		4.1552	3.9192	2.1474
4.3381	4.2045		3.9218	2.1485
		4.2605	4.0036	2.1822
4.4483	4.3101		4.0050	2.1827
4.5366	4.3971		4.0743	2.2112
		4.3780	4.0898	2.2175
4.6440	4.4994		4.1572	2.2451
		4.4856	4.1781	2.2536
		4.5973	4.2659	2.2892
4.7906	4.6424		4.2724	2.2919
4.8795	4.7278		4.3374	2.3181
		4.7387	4.3785	2.3346
4.9540	4.8024		4.3962	2.3417
		4.8750	4.4850	2.3770
5.0999	4.9422		4.5083	2.3862
5.1372	4.9766	4.9378	4.5367	2.3975
		4.9930	4.5814	2.4150
5.3116	5.1419	5.1066	4.6688	2.4491
5.4101	5.2414	5.2045	4.7452	2.4785
5.5124	5.3386	5.3020	4.8233	2.5082
5.6314	5.4547	5.4194	4.9152	2.5426
5.7649	5.5849	5.5516	5.0238	2.5826
5.8263	5.6438	5.6106	5.0703	2.5994
5.9421	5.7619	5.7256	5.1577	2.6305
6.0495	5.8683	5.8349	5.2457	2.6612
6.1314	5.9513	5.9209	5.3125	2.6840
6.2331	6.0563	6.0225	5.3978	2.7126
6.3520	6.1703	6.1408	5.4884	2.7420
6.4172	6.2285	6.2048	5.5404	2.7585
6.4739	6.2861	6.2598	5.5888	2.7736

where (*20*, *27*, *30*). The inner-sphere hydration number change appears to have been confirmed by recent X-ray diffraction measurements (*6*).

The above series trends for the chlorides and perchlorates are modified for the rare earth nitrates since both inner- and outer-sphere ion pairs can form, even in fairly dilute solutions (*1*, *3*, *22*, *24*, *25*). Only for the electrical conductances (*19*), the partial molal heat capacities (*2*, *32*), and, to a lesser extent, for $\gamma_{\pm}$ do actual reversals occur in the series trends due to this complex formation. For most of the other properties the effect

Table III. Coefficients and Powers for Osmotic Coefficient Polynomials

i	r_i	$A_i(La(NO_3)_3)$	$A_i(Pr(NO_3)_3)$	$A_i(Nd(NO_3)_3)$
1	0.750	−4.055 887	−17.597 14	−8.405 083
2	0.875	25.840 87	82.370 45	42.160 13
3	1.000	−19.934 18	−90.784 19	−38.572 79
4	1.250	−6.669 542	40.764 27	3.462 327
5	1.500	12.826 75	−14.447 91	8.724 438
6	1.750	−6.357 021	2.596 327	−5.729 736
7	2.000	1.092 805	−0.144 4624	1.122 014
SD[a]		0.001 3	0.001 1	0.001 3

[a] SD = standard deviation.

of nitrate ion complex formation is to cause moderate distortions to occur in the series trends relative to the behavior at lower concentrations.

Pitzer's equation contains a short range interaction parameter, $3\beta^{(0)}/2$, which seems to contain information about complex formation. The values of $3\beta^{(0)}/2$ are plotted in Figure 7 as a function of the ionic radius (*31*). The values of $3\beta^{(0)}/2$ for $La(NO_3)_3$, $Pr(NO_3)_3$ and $Nd(NO_3)_3$ were taken from Table V, while those for the other salts are from Pitzer et al. (*16*). The $LaCl_3$ value of 0.8334 for $3\beta^{(0)}/2$ appears to have been a misprint for 0.8834. The values of $3\beta^{(0)}/2$ form S-shaped curves as a function of the cation radius for the rare earth chlorides and

Table IV. Osmotic Coefficients, Water Activities, and Activity Coefficients at Even Molalities

m	Φ	a_1	$\gamma\pm$	m	Φ	a_1	$\gamma\pm$
			$La(NO_3)_3$				
0.1	0.7487	0.994620	0.3076	3.0	1.2169	0.7687	0.2949
0.2	0.7503	0.98924	0.2587	3.2	1.2534	0.7490	0.3106
0.3	0.7611	0.98368	0.2368	3.4	1.2896	0.7291	0.3274
0.4	0.7741	0.97793	0.2243	3.6	1.3255	0.7090	0.3454
0.5	0.7879	0.97201	0.2166	3.8	1.3611	0.6889	0.3646
0.6	0.8022	0.96591	0.2116	4.0	1.3962	0.6687	0.3850
0.7	0.8168	0.95963	0.2085	4.2	1.4310	0.6485	0.4068
0.8	0.8318	0.95318	0.2068	4.4	1.4653	0.6284	0.4298
0.9	0.8471	0.94654	0.2060	4.6	1.4991	0.6084	0.4542
1.0	0.8628	0.93972	0.2061	4.8	1.5325	0.5886	0.4801
1.2	0.8951	0.92552	0.2082	5.0	1.5654	0.5689	0.5073
1.4	0.9285	0.91058	0.2123	5.2	1.5978	0.5495	0.5362
1.6	0.9629	0.8949	0.2182	5.4	1.6298	0.5304	0.5666
1.8	0.9981	0.8786	0.2254	5.6	1.6614	0.5115	0.5987
2.0	1.0339	0.8616	0.2341	5.8	1.6926	0.4929	0.6325
2.2	1.0702	0.8439	0.2439	6.0	1.7234	0.4747	0.6681
2.4	1.1068	0.8258	0.2549	6.2	1.7539	0.4567	0.7057
2.6	1.1435	0.8072	0.2671	6.4	1.7841	0.4392	0.7453
2.8	1.1802	0.7881	0.2805	6.4739	1.7952	0.4328	0.7605
			$Pr(NO_3)_3$				
0.1	0.7457	0.994641	0.2956	3.0	1.2757	0.7590	0.3130
0.2	0.7466	0.98930	0.2479	3.2	1.3148	0.7385	0.3317
0.3	0.7575	0.98376	0.2265	3.4	1.3534	0.7178	0.3518
0.4	0.7715	0.97801	0.2146	3.6	1.3915	0.6970	0.3733
0.5	0.7871	0.97204	0.2075	3.8	1.4290	0.6762	0.3963
0.6	0.8038	0.96584	0.2033	4.0	1.4660	0.6554	0.4208
0.7	0.8212	0.95942	0.2009	4.2	1.5025	0.6346	0.4468
0.8	0.8391	0.95278	0.2000	4.4	1.5383	0.6140	0.4745
0.9	0.8575	0.94590	0.2001	4.6	1.5736	0.5936	0.5038
1.0	0.8763	0.93880	0.2011	4.8	1.6083	0.5733	0.5349
1.2	0.9149	0.92394	0.2050	5.0	1.6425	0.5533	0.5678
1.4	0.9543	0.90822	0.2111	5.2	1.6761	0.5336	0.6026
1.6	0.9943	0.8917	0.2189	5.4	1.7091	0.5142	0.6393
1.8	1.0346	0.8744	0.2283	5.6	1.7416	0.4952	0.6781
2.0	1.0752	0.8565	0.2391	5.8	1.7736	0.4765	0.7190
2.2	1.1157	0.8379	0.2513	6.0	1.8051	0.4582	0.7621
2.4	1.1561	0.8188	0.2648	6.2	1.8361	0.4403	0.8075
2.6	1.1963	0.7992	0.2795	6.2861	1.8493	0.4327	0.8278
2.8	1.2362	0.7792	0.2956				
			$Nd(NO_3)_3$				
0.1	0.7391	0.994688	0.2950	3.0	1.3020	0.7547	0.3250
0.2	0.7400	0.98939	0.2462	3.2	1.3417	0.7339	0.3453
0.3	0.7518	0.98388	0.2246	3.4	1.3805	0.7130	0.3669
0.4	0.7671	0.97813	0.2128	3.6	1.4185	0.6921	0.3899
0.5	0.7840	0.97215	0.2059	3.8	1.4556	0.6713	0.4143
0.6	0.8020	0.96592	0.2018	4.0	1.4919	0.6505	0.4402
0.7	0.8208	0.95944	0.1998	4.2	1.5274	0.6298	0.4676
0.8	0.8402	0.95272	0.1991	4.4	1.5622	0.6094	0.4965
0.9	0.8600	0.94575	0.1995	4.6	1.5962	0.5891	0.5271
1.0	0.8803	0.93853	0.2008	4.8	1.6295	0.5691	0.5593
1.2	0.9218	0.92338	0.2056	5.0	1.6622	0.5494	0.5934
1.4	0.9642	0.90731	0.2126	5.2	1.6943	0.5300	0.6292
1.6	1.0071	0.8904	0.2215	5.4	1.7259	0.5109	0.6671
1.8	1.0503	0.8726	0.2320	5.6	1.7571	0.4921	0.7070
2.0	1.0934	0.8542	0.2441	5.8	1.7879	0.4737	0.7492
2.2	1.1362	0.8352	0.2575	6.0	1.8184	0.4556	0.7938
2.4	1.1786	0.8156	0.2724	6.2	1.8488	0.4378	0.8409
2.6	1.2204	0.7956	0.2886	6.2598	1.8578	0.4326	0.8555
2.8	1.2616	0.7753	0.3061				

Table V. Parameters for Pitzer's Equation

parameter	$La(NO_3)_3$	$Pr(NO_3)_3$	$Nd(NO_3)_3$
$3\beta^{(0)}/2$	0.7169	0.7095	0.7023
$3\beta^{(1)}/2$	7.700	7.700	7.700
$(3^{3/2}/2)C^{\Phi}$	−0.1684	−0.1524	−0.1427
SD[a]	0.0097	0.0073	0.0077

[a] SD = standard deviation.

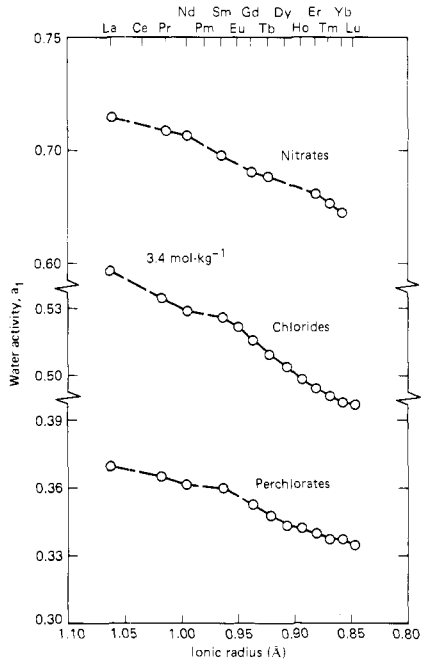

Figure 6. Water activities of rare earth chlorides, perchlorates, and nitrates at 3.4 mol kg^{-1}.

perchlorates, and this behavior can be attributed to cation hydration trends. For the rare earth nitrates, $3\beta^{(0)}/2$ decreases from La to Sm and then increases for the remaining rare earths.

The radius dependence of the $3\beta^{(0)}/2$ values for the rare earth nitrates suggests that complex formation increases from La to Sm at low concentrations and then decreases for the heavy rare earths. This behavior is consistent with stability constant values (*4*, *13*, *15*) and electrical conductance data (*19*). These electrical conductances indicate that this maximum in complex formation disappears by 0.8–0.9 mol kg^{-1}, and at higher concentrations the amount of complex formation decreases from La to Lu. The activity data are in agreement with these stability constant trends. In addition, cation hydration numbers for the rare earth nitrates should increase as the amount of complex formation decreases. Hydration numbers from ultrasonic absorption measurements approximately show this behavior (*9*).

All of the thermodynamic (*2*, *9*, *26*, *28*, *32*) and transport data (*19*, *29*) for the rare earth nitrates exhibit some type of "bulge" in the middle of the series at moderate and high concentrations. This "bulge" must have some structural significance in terms of changes in nitrate ion and/or water coordination. However, the detailed nature of this change is presently unknown. Additional Raman spectral measurements (*5*, *14*) and ultrasonic absorption mechanism studies (*24*, *25*) could help to clarify this situation.

Activity data have now been reported for a total of 35 aqueous rare earth electrolytes up to saturation or supersaturation at 25 °C. These data will be valuable, together with available data for salts of other valence types, for use in attempts to find theoretical and empirical relationships between the activities and ionic radii, charge type, and amount of complex formation. Data for rare earth salts are also being measured at the Technical University of Gdansk (*12*).

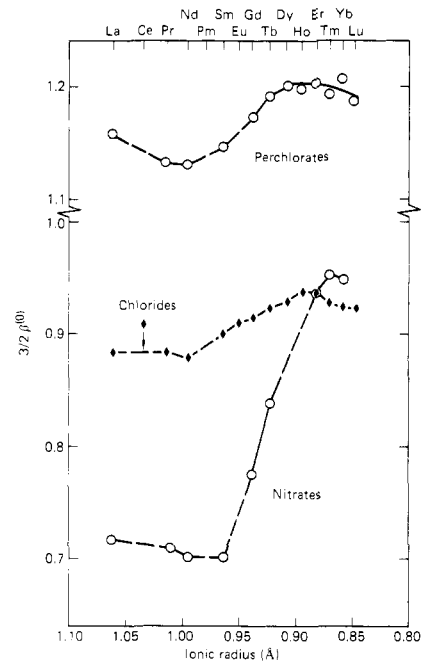

Figure 7. Pitzer's pairwise short-range interaction parameter, $3\beta^{(0)}/2$, for rare earth chlorides, perchlorates, and nitrates.

Acknowledgment

The authors thank Anton Habenschuss (Ames Laboratory) for assistance with the least-squares calculations.

Glossary

Φ	molal osmotic coefficient
ν	number of ions formed by the dissociation of one molecule of solute
m	molal concentration, mol kg^{-1}, of the solute
$\gamma_{\pm}$	mean molal activity coefficient
a_1	water activity
$\beta^{(0)}$, $\beta^{(1)}$, C^{Φ}	parameters for Pitzer's equation

Literature Cited

(1) Abrahamer, I., Marcus, Y., *Inorg. Chem.*, **6**, 2103 (1967).
(2) Baker, J. L., unpublished Ph.D. dissertation, Iowa State University, Ames, Iowa, 1971.
(3) Choppin, G. R., Henrie, D. E., Buijs, K., *Inorg. Chem.*, **5**, 1743 (1966).
(4) Choppin, G. R., Strazik, W. F., *Inorg. Chem.*, **4**, 1250 (1965).
(5) Egorov, V. N., Kuzinets, I. E., *Russ. J. Inorg. Chem.*, **22**, 681 (1977).
(6) Habenschuss, A., Spedding, F. H., *J. Chem. Phys.*, **70**, 2797, 3758 (1979).
(7) Hall, R. E., Harkins, W. D., *J. Am. Chem. Soc.*, **38**, 2658 (1916).
(8) Hamer, W. J., Wu, Y.-C., *J. Phys. Chem. Ref. Data*, **1**, 1047 (1972).
(9) Jezowska-Trzebiatowska, B., Ernst, S., Legendziewicz, J., Oczko, G., *Bull. Acad. Pol. Sci., Ser. Sci. Chim.*, **24**, 997 (1976); **25**, 649 (1977).
(10) Jones, H. C., Getman, F. H., *Z. Phys. Chem.*, **46**, 244 (1903).
(11) Kirgintsev, A. N., Luk'yanov, A. V., *Russ. J. Phys. Chem.*, **39**, 389 (1965).
(12) Libuś, Z., private communication.
(13) Moulin, N., Hussonnois, M., Brillard, L., Guillaumont, R., *J. Inorg. Nucl. Chem.*, **37**, 2521 (1975).
(14) Nelson, D. L., Irish, D. E., *J. Chem. Phys.*, **54**, 4479 (1971); *J. Chem. Soc., Faraday Trans. 1*, **69**, 156 (1973).
(15) Peppard, D. F., Mason, G. W., Hucher, I., *J. Inorg. Nucl. Chem.*, **24**, 881 (1962).
(16) Pitzer, K. S., Peterson, J. R., Silverster, L. F., *J. Solution Chem.*, **7**, 45 (1978).
(17) Rard, J. A., Habenschuss, A., Spedding, F. H., *J. Chem. Eng. Data*, **22**, 180 (1977).
(18) Rard, J. A., Shiers, L. E., Heiser, D. J., Spedding, F. H., *J. Chem. Eng. Data*, **22**, 337 (1977).
(19) Rard, J. A., Spedding, F. H., *J. Phys. Chem.*, **79**, 257 (1975).
(20) Rard, J. A., Weber, H. O., Spedding, F. H., *J. Chem. Eng. Data*, **22**, 187 (1977).
(21) Reidler, J., Silber, H. B., *J. Inorg. Nucl. Chem.*, **36**, 175 (1974).
(22) Reuben, J., Fiat, D., *J. Chem. Phys.*, **51**, 4909 (1969).
(23) Sayre, E. V., Miller, D. G., Freed, S., *J. Chem. Phys.*, **26**, 109 (1957).
(24) Silber, H. B., Fowler, J., *J. Phys. Chem.*, **80**, 1451 (1976).
(25) Silber, H. B., Scheinin, N., Atkinson, G., Grecsek, J. J., *J. Chem. Soc., Faraday Trans. 1*, **68**, 1200 (1972).

(26) Spedding, F. H., Derer, J. L., Mohs, M. A., Rard, J. A., J. Chem. Eng. Data, 21, 474 (1976).
(27) Spedding, F. H., Rard, J. A., Habenschuss, A., J. Phys. Chem., 81, 1069 (1977).
(28) Spedding, F. H., Shiers, L. E., Brown, M. A., Baker, J. L., Gutierrez, L., McDowell, L. S., Habenschuss, A., J. Phys. Chem., 79, 1087 (1975).
(29) Spedding, F. H., Shiers, L. E., Rard, J. A., J. Chem. Eng. Data, 20, 88 (1975).
(30) Spedding, F. H., Weber, H. O., Saeger, V. W., Petheram, H. H., Rard, J. A., Habenschuss, A., J. Chem. Eng. Data, 21, 341 (1976).
(31) Templeton, D. H., Dauben, C. H., J. Am. Chem. Soc., 78, 5237 (1954).
(32) Walters, J. P., Spedding, F. H., IS-1988, unclassified U.S.A.E.C. Report, 1968.

Received for review March 19, 1979. Accepted June 25, 1979. J.A.R. was supported by the National Science Foundation Earth Science Grant No. EAR76-20149 (coprincipal investigators Donald Graf and David Anderson, Geology Department, University of Illinois at Urbana—Champaign). The authors wish to thank Lawrence Livermore Laboratory for partial support of this project. Work performed in part under the auspices of the U.S. Department of Energy by the Lawrence Livermore Laboratory under Contract No. W-7405-ENG-48.

Pressure and Temperature Dependence of the Diffusion of Methane in Helium

Frank J. Yang* and Stephen J. Hawkes

Department of Chemistry, Oregon State University, Corvallis, Oregon 97331

Values of the binary molecular diffusion coefficient, D_{12}, for CH_4 in He are obtained at atmospheric pressure and temperatures from 283 to 343 K and also at pressures from 47 to 112 atm at 303 K, with an uncertainty of 0.2%. Within this experimental uncertainty, D_{12} was linear with gas density. It fitted the equations log D_{12} = −4.3256 + 1.6783 log T and also the Lennard-Jones 12-6 formula using the fitted values ϵ_{12}/k = 40.8 K and σ_{12} = 3.186 A.

Experimental Section

The basic gas chromatographic system has been previously described (*1*). However, in the pressure-dependence studies, Nupro precision valves (Nupro Co., Cleveland, Ohio) both at the inlet and the outlet of the column were replaced by a pressure regulator (Consolidated Controls, Calif.) and a specially designed high-pressure control valve developed in Dr. J. C. Giddings' Laboratories, University of Utah, respectively.

The continuous elution gas chromatographic method employed here follows the same general procudure as in our previous report (*1*).

Helium gas (99.995% purity; Matheson Gas Products) was used as carrier gas. Flow rates were in the range 1.56–1.73 cm/s for the temperature-dependence studies and in the range of 0.95–1.02 cm/s for pressure-dependence studies. The methane was Matheson C.P. grade with a minimum purity of 99.0%. Since the accuracy of our measurements was better than 1%, this is a lower purity than desirable but fortunately the most likely impurity is hydrogen which is invisible to the flame ionization detector used and so has no effect on the result. If there were 1.0% of ethane present, our results would be $^1/_4$% low which is about the limit of our experimental reliability. Hence the 99.0% purity of the methane is adequate.

Trace amounts of methane gas were injected directly into the column by a specially designed sampling valve (*1*). The sample chamber had been pressurized up to the same pressure as that of the column before the injection of sample occurred.

A 316 stainless steel column with a measured (*1*) effective length of 461.98 cm and a radius of 0.110 cm was employed.

In the temperature-dependence studies pressure at the inlet of the column was controlled at 1.743 ± 0.0015 atm and the temperature was in the range of (10–60) ± 0.02 °C. The pressure gradient across the column was 0.002 atm, measured by using a 1.0-psi differential pressure transducer (Model KP 15, Whittaker Corp., North Hollywood, Calif.). Column pressure was measured by a mercury barometer at the outlet of the column.

In pressure dependence studies, the pressure was set between 700 and 1640 psi and the temperature was set at 30 ± 0.02 °C. Column pressure was measured by both an absolute pressure transducer (Model P2A, Whittaker Corp., Calif.) and a pressure gage (range 0–4000 psi; American Instrument Co., Inc., Silver Spring, Md.).

Sample eluted from the column was detected by a flame ionization detector. The current source from the FID was converted to voltage and amplified to about 1 V and then collected directly through a computer interfacing system to the disk memory system of the CDC computer at Oregon State University.

Four or more separate runs were conducted for each experimental condition. About 1000 data points were collected for each elution peak. The area, moments, skewness, kurtosis, velocity, and dispersion coefficient were determined numerically. The data points were then assembled into about 200 points by using a sequential 7 to 11 data points average routine. These were fitted to the theoretical equation (eq 1), where C is the

$$C = \frac{C_0 L}{2\left[\pi\left(\frac{D_{12}}{p} + \frac{r^2 v^2 p}{48 D_{12}}\right)\right]^{1/2} t^{3/2}} \times \exp\left\{-\frac{(L - Vt)^2}{4t\left(\frac{D_1}{p} + \frac{r^2 v^2 p}{48 D_{12}}\right)}\right\} \quad (1)$$

instantaneous concentration at the exit of the column at time t, C_0 is the initial concentration at the inlet of the column, L is the column length, r is the column radius, v is the average linear flow velocity, t is the elution time, and p is the column pressure in atm.

Results and Discussion

Temperature Dependence. Table I gives the average value of the diffusion coefficients of the helium–methane gas pair obtained at 10, 15, 20, 25, 30, 40, 50, 55, and 60 °C. The

* To whom correspondence should be addressed at the Varian Instrument Division, GC Research Department, 2700 Mitchell Drive, Walnut Creek, California 94598.

0021-9568/79/1724-0354$01.00/0